Organometallics 1991, *10*, 143–148

Dinuclear Cyclopentadienyl Carbonyl and Alkyne Complexes of Niobium(II) and Tantalum(II). Structures of $[(C_5H_4Me)Nb(\mu\text{-}Cl)(CO)_2]_2$, $[(C_5H_4Me)Nb(\mu\text{-}Cl)(ArC{\equiv}CAr)]_2$, and $[(C_5Me_5)Ta(\mu\text{-}Cl)(CO)_2]_2$

Daekeun Kwon, Julio Real, and M. David Curtis*

Department of Chemistry, The University of Michigan, Ann Arbor, Michigan 48109-1055

Arnold Rheingold and Brian S. Haggerty

Department of Chemistry, The University of Delaware, Newark, Delaware 19716

Received April 30, 1990

The M(III) complexes (M = Nb, Ta) $[(\eta^5\text{-}C_5H_4Me)NbCl(\mu\text{-}Cl)(CO)_2]_2$, $(\eta^5\text{-}C_5H_4Me)NbCl_2(ArCCAr)$, and $[(\eta^5\text{-}C_5Me_5)TaCl_2(CO)_2(THF)$ were reduced with Na/Hg to give diamagnetic M(II) dinuclear complexes with M–M bonds: $[(\eta^5\text{-}C_5H_4Me)Nb(\mu\text{-}Cl)(CO)_2]_2$ (**1**), $[(\eta^5\text{-}C_5H_4Me)Nb(\mu\text{-}Cl)(ArCCAr)]_2$ (**2a**), and $[(\eta^5\text{-}C_5Me_5)Ta(\mu\text{-}Cl)(CO)_2]_2$ (**3**), respectively (Ar = 4-methylphenyl). The structures of **1**, **2a**, and **3** were determined by single-crystal X-ray diffractometry. Crystal data for **1**: space group $P\bar{1}$, $Z = 2$, $a = 10.279$ (3) Å, $b = 11.247$ (3) Å, $c = 8.587$ (2) Å, $V = 904.6$ (4) Å^3, $R = 0.031$, $R_w = 0.034$ based on 2667 reflections with $I > 3\sigma(I)$. Crystal data for **2a**: space group $P\bar{1}$, $Z = 1$, $a = 9.623$ (3) Å, $b = 9.781$ (3) Å, $c = 12.245$ (4) Å, $V = 933.5$ (6) Å^3, $R = 0.032$, $R_w = 0.031$ based on 2710 reflections with $I > 3\sigma(I)$. Crystal data for **3**: space group $P2_1/n$, $Z = 4$, $a = 8.660$ (2) Å, $b = 14.790$ (3) Å, $c = 21.009$ (7) Å, $\beta = 98.81$ (2)°, $V = 2659.7$ (16) Å^3, $R = 0.039$, $R_w = 0.041$ based on 3816 reflections with $I > 3\sigma(I)$. The structures of carbonyl complexes **1** and **3** and alkyne complex **2a** are considerably different; **1** and **3** have folded M_2Cl_2 cores, whereas **2a** has a centrosymmetric structure with a planar M_2Cl_2 core.

Introduction

The chemistry of metal–metal multiple bonds for group V metal complexes is not well developed. Possible synthetic schemes for multiply bonded complexes are reductive coupling of monomeric precursors or further reduction of dimeric complexes in intermediate oxidation states. There are a number of early reports on reductive dimerization that yield lower valent dinuclear adducts of niobium and tantalum.[1] Previously reported niobium(II) and tantalum(II) species include phosphine complexes MCl_2L_4[2a] and aryloxides $L_4M(OAr)_2$.[2b] Sattelberger et al.[3] have shown that these complexes oxidatively add molecular hydrogen to afford the paramagnetic M(IV) dihydrides $MCl_2H_2L_4$. Cotton et al. have prepared confacial, bioctahedral Nb(II) and Ta(II) dimers of the type $M_2X_6L_3{}^{2-}$ that feature triply bonded metals by reduction of $M_2X_6L_3$ precursors.[4]

Organometallic complexes of Nb(II) or Ta(II) are extremely rare. The heterometallic dimers Cp_2NbM' (M′ = $Mo(CO)_3Cp$,[5] $FeH(CO)_4$,[6] $Co(CO)_4$[7]) can be considered Nb(II) compounds, but they can be viewed also as containing Cp_2Nb^+ (niobium(III)), coupled with the anionic M'^- moiety. Bunker and Green[8] have reported that $CpNbCl_2(Me_4C_4H_2)$ ($Me_4C_4H_2$ = 1,2,3,4-tetramethylbuta-1,3-diene) is reduced by sodium amalgam to $[CpNb(\mu\text{-}Cl)_2(Me_4C_4H_2)]_2$. This Nb(II) dimer was characterized crystallographically and reported to have a planar Nb_2Cl_2 core, but no other details were provided. Recently, Wexler and Wigley reported novel $(\eta^6\text{-}C_6R_6)Ta(OR')_2$ derivatives.[9]

Here, we report syntheses of new, low-valent organometallic complexes of Nb and Ta as a part of our research into metal–metal multiple-bonded complexes of the group V metals. Some of these results have been communicated in preliminary form.[10b] (Note: unless explicitly denoted otherwise, the abbreviations Cp = C_5H_5, Cp′ = C_5H_4Me, Cp* = C_5Me_5, and Ar = 4-methylphenyl will be used throughout this paper.)

Experimental Section

All operations were carried out under dinitrogen with use of standard Schlenk techniques or an inert-atmosphere box equipped with a purifier train. Elemental analyses were performed by The University of Michigan microanalytical service or by Galbraith Laboratories, Inc. (Knoxville, TN). Infrared measurements were made on a Nicolet 5DXB or Perkin-Elmer Model 1330 spectrometer. Mass spectra were obtained on a Finnigan Model 4021 GC–MS or VG 70-250s spectrometer. Nuclear magnetic resonance spectra were run on a Bruker AM-300 instrument (operating at 300 MHz for ^{1}H and 75.5 MHz for ^{13}C). The ^{1}H and ^{13}C NMR spectra were referenced to TMS. Niobium and tantalum pentachloride were purchased from Pressure Chemical Co. and stored in the glovebox. Solvents were dried by standard procedures and degassed prior to use.

Synthesis of $[Cp'Nb(\mu\text{-}Cl)(CO)_2]_2$ (1). A solution of 4.60 g (7.7 mmol) of $[Cp'NbCl_2(CO)_2]_2$[10] in 120 mL of THF was placed in a 250-mL Morton flask and stirred vigorously. To this solution was added 220 g of sodium amalgam (0.16% Na/Hg (w/w), 15.4 mmol of Na). Some gas evolution was observed, and the solution changed from cherry red to very dark brown immediately. White sodium chloride was observed to precipitate. After it was stirred for 1 h, the solution was filtered through a 2-cm layer of Celite and the THF stripped off to yield a brown-black oily residue. The

---

[1] Messerle, L. *Chem. Rev.* 1988, *88*, 1229.

[2] (a) Datta, S.; Wreford, S. S. *Inorg. Chem.* 1977, *16*, 1134. (b) Coffindaffer, T. W.; Rothwell, I. P.; Folting, K.; Huffman, J. C.; Streib, W. E. *J. Chem. Soc., Chem. Commun.* 1985, 1519.

[3] Luetkens, M. L., Jr.; Elcesser, W. L.; Huffmann, J. C.; Sattelberger, A. P. *Inorg. Chem.* 1984, *23*, 1718.

[4] Cotton, F. A.; Diebold, M. P.; Roth, W. J. *J. Am. Chem. Soc.* 1987, *109*, 5506.

[5] Pasynskii, A. A.; Shrtipkin, Yu. V.; Eremenko, I. L.; Kalimnikov, V. T.; Aleskandrov, G. G.; Adrianov, V. G.; Struchkov, Yu. T. *J. Organomet. Chem.* 1979, *165*, 49.

[6] Wong, K. S.; Scheidt, W. R.; Labinger, J. A. *Inorg. Chem.* 1979, *18*, 136.

[7] Wong, K. S.; Scheidt, W. R.; Labinger, J. A. *Inorg. Chem.* 1979, *18*, 1709.

[8] Bunker, M. J.; Green, M. L. H. *J. Chem. Soc., Dalton Trans.* 1981, 85.

[9] Wexler, P. A.; Wigley, D. E. *J. Chem. Soc., Chem. Commun.* 1989, 664.

[10] (a) Curtis, M. D.; Real, J.; Kwon, D. *Organometallics* 1989, *8*, 1644. (b) Curtis, M. D.; Real, J. *Organometallics* 1985, *4*, 940.

0276-7333/91/2310-0143$02.50/0

Table I. Crystallographic Data for [Cp′Nb(μ-Cl)(CO)$_2$]$_2$ (1), [Cp′Nb(μ-Cl)(MePhC≡CPhMe)]$_2$ (2a), and [Cp*Ta(μ-Cl)(CO)$_2$]$_2$ (3)

formula	$C_{16}H_{14}Cl_2Nb_2O_4$	$C_{44}H_{42}Cl_2Nb_2$	$C_{24}H_{30}Cl_2O_4Ta_2$
mol wt	527	827	815.302
color	dark brown	dark mustard brown	brown-black
space group	$P\bar{1}$	$P\bar{1}$	$P2_1/n$
a, b, c, Å	10.279 (3), 11.247 (3), 8.587 (2)	9.623 (3), 9.781 (3), 12.245 (4)	8.660 (2), 14.790 (3), 21.009 (7)
α, β, γ, deg	100.59 (2), 111.01 (2), 79.95 (2)	96.20 (3), 113.19 (3), 62.24 (2)	90, 98.81 (2), 90
cell vol, Å^3	904.6 (4)	933.5 (6)	2659.7 (16)
Z	2	1	4
calcd density, g/cm^3	1.94	1.47	2.036
cryst dimens, mm	0.24 × 0.28 × 0.20	0.120 × 0.407 × 0.225	0.18 × 0.18 × 0.36
2θ limit, deg	50	45	52
no. of unique data	3429	3310	5230
no. of obsd data ($I > 3\sigma(I)$)	2667	2710	3816
largest residual, e/Å^3	0.45	0.29	1.5
R	0.031	0.032	0.039
R_w	0.034	0.031	0.041
goodness of fit	1.54	0.91	1.129

residue was extracted with ca. 300 mL of toluene and an insoluble black material removed by filtration. The filtrate was concentrated to ca. 50 mL, and an equal volume of octane was added. The product was allowed to crystallize overnight. The dark brown microcrystalline product was collected by filtration, washed with hexane (3 × 5 mL), and vacuum-dried. A second crop was obtained by concentration of the filtrate and cooling. The two crops were combined and recrystallized from toluene/hexane; yield 1.46 g (36%) of dark brown 1. ^{1}H NMR (C_7D_8): δ 4.72, 4.46 (m, m, A_2B_2, 4 H, $C_5\mathit{H}_4$Me), 1.69 (s, 3 H, $CpC\mathit{H}_3$). ^{13}C{^{1}H} NMR (C_7D_8): δ 116.6, 95.9, 88.9, (C_5H_5Me), 14.8 ($CpCH_3$). IR (CH_2Cl_2, cm^{-1}): 1990 (st), 1910 (st). Mass spectrum (CI, methane): *m/e* 526 [M]$^+$ (Cl_2 pattern), 498 [M − (CO)]$^+$, 470 [M − (CO)$_2$]$^+$, 442 [M − (CO)$_3$]$^+$, 414 [M − (CO)$_4$]$^+$, 270 [MeCpNbCl]$^+$. Anal. Calcd for $C_{16}H_{14}Cl_2Nb_2O_4$: C, 36.47; H, 2.68; Cl, 13.45. Found: C, 36.52; H, 2.76; Cl, 13.39.

Syntheses of [CpNb(μ-Cl)(ArC≡CAr)]$_2$ (2). Two derivatives were prepared: Cp = C_5H_4Me (**2a**) and Cp = C_5H_5 (**2b**). The same method was used for both with similar results. The preparation is described for **2a**.

A solution of 0.80 g (1.79 mmol) of Cp′NbCl$_2$(ArC≡CAr)[10] in 50 mL of toluene was cooled to −8 °C and treated with 2.0 mL of sodium amalgam (1.90 mmol of Na, 0.162% Na/Hg (w/w)). The mixture turned dark olive green, and sodium chloride was observed to precipitate. After the solution was stirred for 24 h at −8 °C, a small amount of Darco activated charcoal was added and the solution filtered through a 2-cm layer of Celite. The clear, dark green-brown filtrate was concentrated to a volume of ca. 2 mL, at which point crystals started to form; the solution was layered with hexane (5 mL) and allowed to rest. A crop of crystals formed; then 50 mL of hexane was added and the solution allowed to rest at −8 °C for 4 h. The crystals were collected by filtration, washed with hexane (4 × 2 mL), and vacuum-dried. The filtrate was concentrated to a volume of ca. 0.5 mL and layered with hexane (ca. 5 mL), and a second crop of crystals was obtained and isolated as before. The two crops were combined and recrystallized from toluene/hexane; yield 0.64 g (86%) of **2a**. Note: while crystals are dark mustard brown, powdered **2a**,**b** are olive green. **2a**: ^{1}H NMR (C_6D_6) δ 7.73, 7.14 (d, d, pseudo-A_2B_2, J = 8 Hz, 8 H, $C_6\mathit{H}_4$Me), 5.20, 4.86 (m, m, AA′BB′, 4 H, $C_5\mathit{H}_4$Me), 2.16 (s, 6 H, $ArC\mathit{H}_3$), 1.42 (s, 3 H, $CpC\mathit{H}_3$); ^{13}C{^{1}H} NMR (C_6D_6): δ 213.9 (Ar*C*≡*C*Ar), 138.5, 137.4, 129.4, 128.8 (C_6H_4Me) 122.3, 102.1, 99.6 (C_5H_4Me), 21.4 ($ArCH_3$), 14.7 ($Cp\mathit{C}H_3$). Anal. Calcd for $C_{44}H_{42}Cl_2Nb_2$: C, 63.86; H, 5.12; Cl, 8.57. Found: C, 64.15; H, 5.38; Cl, 8.39. **2b**: ^{1}H NMR (C_6D_6) δ 7.64, 7.12 (d, d, pseudo-A_2B_2, J = 8 Hz, 8 H, $C_6\mathit{H}_4$Me), 5.14 (s, 5 H, $C_5\mathit{H}_5$), 2.16 (s, 6 H, $ArC\mathit{H}_3$); ^{13}C{^{1}H} NMR (C_6D_6) δ 216.4 (Ar*C*≡*C*Ar), 138.7, 137.5, 129.5, 128.5 (C_6H_4Me), 102.8 (C_5H_5), 21.3 ($ArCH_3$).

Synthesis of [Cp*Ta(μ-Cl)(CO)$_2$]$_2$ (3). A solution of 3.00 g (5.82 mmol) of Cp*TaCl$_2$(CO)$_2$(THF)[9] was cooled to −8 °C and treated with sodium amalgam (0.2 g of Na, 8.7 mmol). The mixture slowly turned dark brown. After it was stirred for 1 day at −8 °C, the solution was filtered through a layer of Celite. The yellow-brown filtrate was concentrated to give dark brown crystals. More crystalline solids were obtained by layering with hexane. The product was washed with hexane and dried; yield 1.7 g (71%). ^{1}H NMR (C_6D_6): δ 1.74 (s, $C_5\mathit{Me}_5$). ^{13}C{^{1}H} NMR (C_6D_6): δ 103.2 (C_5Me$_5$), 11.3 ($C_5\mathit{Me}_5$). IR (THF, cm^{-1}): 1976 (st), 1893 (st). IR (CH_2Cl_2, cm^{-1}): 1974 (st), 1888 (st). Mass spectrum (EI, 70 eV): *m/e* 814 [M]$^+$ (Cl_2 pattern), 787 [M − (CO) + 1]$^+$, 758 [M − (CO)$_2$]$^+$. Anal. Calcd for $C_{24}H_{30}Cl_2O_4Ta_2$: C, 35.36; H, 3.71. Found: C, 35.04; H, 3.66.

Crystallographic Analysis for 1 and 3. Crystallographic data are collected in Table I. The X-ray study was carried out by using a Syntex P2$_1$ automatic diffractometer. Intensity data were obtained by variable-rate θ–2θ scans with Mo Kα radiation (λ = 0.710 69 Å, graphite monochromator). Lattice parameters were obtained by a least-squares analysis of 15 reflections scattered in reciprocal space, obtained from the automatic centering routine. Intensities of three standard reflections were monitored after every 50 data points. Background was measured before and after each peak; the background to scan time ratio was ca. 1.0. The solution and refinement of the structure were carried out on an IBM 3090/600E computer using the SHELX package that includes subroutines for direct methods, difference Fourier maps, least-squares refinements, and distance and angle calculations. The atomic scattering factors were taken from ref 18. The data were corrected for Lorentz and polarization effects. The structures were solved by direct methods and refined by standard least-squares and difference Fourier methods. The function minimized by the least-squares program was $w(F_o - F_c)^2$ with the weights, w, assigned as $1/(\sigma^2F_o + 10^{-4}F_o^2)$.

A dark brown crystal for X-ray diffraction was selected from the crop of crystals obtained from a dichloromethane/hexane solution of 1. A Patterson map revealed the positions of the two niobium atoms, and subsequent least-squares refinements and difference Fourier maps gave the positions of all non-hydrogen atoms. All non-hydrogen atoms were refined anisotropically. Hydrogens were included in the last refinement in calculated positions with fixed isotropic temperature factors. An absorption correction was not necessary. In the structure of 1, the molecule lies in a general position and has no crystallographic symmetry. The idealized symmetry is C_{2v}, which makes the halves of the dimer equivalent.

Crystals of **2a** were grown from a toluene solution layered with hexane. A suitable crystal was sealed in a thin-walled capillary and mounted on the diffractometer. Intensity statistics suggested the centric space group $P\bar{1}$ rather than noncentric $P1$. The position of the niobium atom was obtained by direct methods, and the rest of the non-hydrogen atoms were revealed by subsequent least-squares refinements and difference Fourier maps. All non-hydrogen atoms were refined anisotropically. Hydrogens were included in fixed calculated positions with fixed isotropic temperature factors. An absorption correction was not necessary. In the crystal, the dimer **2a** sits on a crystallographic inversion center at the midpoint of the Nb–Nb′ bond that makes the halves of the molecule identical. Although strictly C_i, the idealized symmetry of the molecule is C_{2h}.

Methods used in the data collection for **3** are similar to those used for 1 and **2a**, except that a Nicolet R3m/μ diffractometer was used for data collection and SHELXTL (5.1) software was executed on a Data General S-30 computer. Brown-black crystals

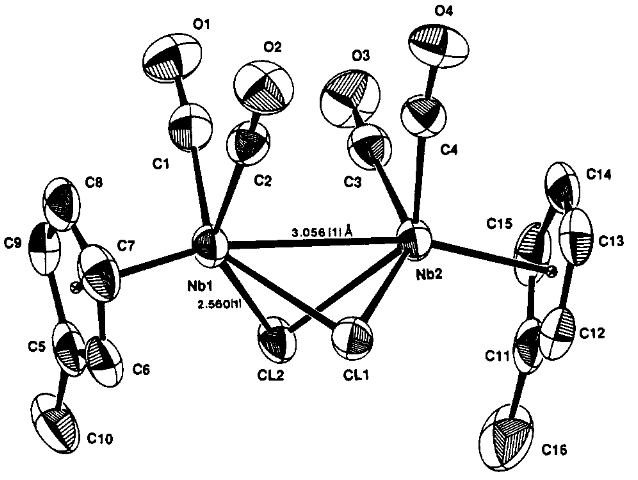

Figure 1. ORTEP plot (50% probability thermal ellipsoids) of the molecular structure of $[(C_5H_4Me)Nb(\mu\text{-}Cl)(CO)_2]_2$ (1) with the numbering scheme.

of 3 for X-ray diffraction were grown by slow evaporation of a toluene solution under an atmosphere of purified nitrogen. The space group for 3, $P2_1/n$, was uniquely determined from systematic absences and axial photographs. The data were corrected for absorption by an empirical procedure. The Ta atoms were located by direct methods. All non-hydrogen atoms were refined with anisotropic thermal parameters; hydrogen atoms were ignored.

Results and Discussion

Recently, we reported that $CpCl_2Nb^{III}$ compounds were prepared by reduction of $CpNbCl_4$ with $Al/HgCl_2$ in the presence of suitable ligands:[10]

$$CpNbCl_4 + L \xrightarrow[THF]{Al/HgCl_2} CpNbCl_2L \qquad (1)$$

$$L = 2CO,\ ArCCAr$$

The niobium(III) complexes $[Cp'NbCl(\mu\text{-}Cl)(CO)_2]_2$ and $CpNbCl_2(ArCCAr)$ were reduced by sodium amalgam to afford the novel Nb(II) homometallic dimers $[Cp'Nb(\mu\text{-}Cl)(CO)_2]_2$ (1) in 36% yield and $[RNb(\mu\text{-}Cl)(ArC{\equiv}CAr)]_2$ (R = Cp′ (**2a**), C_5H_5 (**2b**)) in 80% yield, according to eqs 2 and 3.

$$[Cp'NbCl(\mu\text{-}Cl)(CO)_2]_2 \xrightarrow{Na/Hg} [Cp'Nb(\mu\text{-}Cl)(CO)_2]_2 \qquad (2)$$

$$2CpNbCl_2(ArCCAr) \xrightarrow{2Na/Hg} [CpNb(\mu\text{-}Cl)(ArCCAr)]_2 \qquad (3)$$
$$\mathbf{2a},\ Cp = C_5H_4Me$$
$$\mathbf{2b},\ Cp = C_5H_5$$

The higher yield obtained in the reduction of the alkyne complexes is explained by their higher thermal stability compared to that of the carbonyl complexes.

In the ^1H NMR spectrum, complex 1 exhibits equivalent Cp′ groups. In the infrared spectrum, the ν_{CO} frequencies (1990 and 1910 cm^{-1}) are characteristic of terminal carbonyl ligands. In the ^{13}C NMR spectrum of 1, the carbonyl carbon resonances were not observed. This can be explained by the high quadrupole moment of the niobium nucleus and the short Nb–CO distance (ca. 2.10 Å). However, the alkyne carbon resonances of the niobium alkyne complexes prepared in this work were always observed, although they were of low intensity and were somewhat broad.

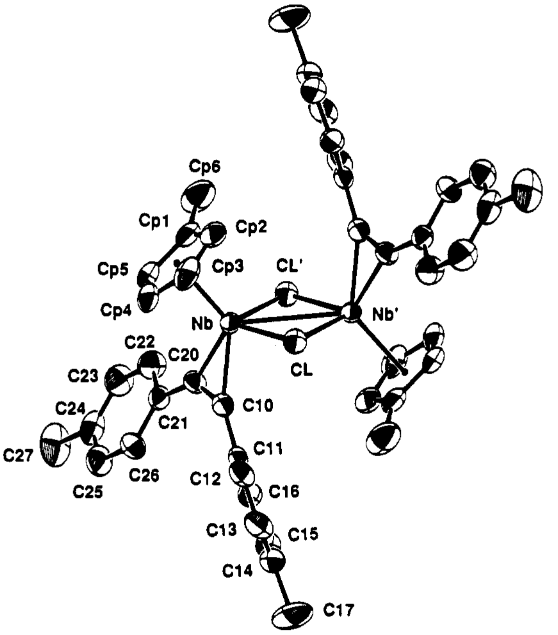

Figure 2. ORTEP plot (50% probability thermal ellipsoids) of the molecular structure of $[(C_5H_4Me)Nb(\mu\text{-}Cl)(ArC{\equiv}CAr)]_2$ (2) with the numbering scheme.

Table II. Fractional Atomic Coordinates for $[Cp'Nb(\mu\text{-}Cl)(CO)_2]_2$ (1)

atom	*x*	*y*	*z*
Nb1	0.18014 (4)	0.20380 (3)	-0.13597 (5)
Nb2	0.32917 (4)	0.33409 (3)	-0.29392 (5)
Cl1	0.44088 (12)	0.23224 (11)	-0.02471 (16)
Cl2	0.26944 (14)	0.11446 (10)	-0.38072 (16)
C1	-0.0012 (6)	0.2853 (5)	-0.2989 (6)
O1	-0.1088 (4)	0.3294 (4)	-0.3776 (5)
C2	0.1599 (5)	0.3658 (5)	0.0202 (6)
O2	0.1452 (5)	0.4500 (4)	0.1100 (5)
C3	0.1397 (6)	0.3644 (5)	-0.4904 (7)
O3	0.0418 (4)	0.3812 (4)	-0.6012 (5)
C4	0.2509 (5)	0.4906 (5)	-0.1720 (6)
O4	0.2123 (4)	0.5830 (3)	-0.1162 (5)
C5	0.1424 (6)	-0.0066 (5)	-0.1396 (7)
C6	0.2333 (6)	0.0327 (5)	0.0200 (7)
C7	0.1630 (6)	0.1325 (5)	0.0945 (7)
C8	0.0266 (7)	0.1571 (5)	-0.0205 (8)
C9	0.0122 (6)	0.0729 (5)	-0.1697 (8)
C10	0.1684 (7)	-0.1146 (5)	-0.2606 (8)
C11	0.5107 (6)	0.2879 (5)	-0.4226 (7)
C12	0.5694 (5)	0.3481 (5)	-0.2624 (7)
C13	0.4974 (6)	0.4643 (5)	-0.2494 (7)
C14	0.3925 (6)	0.4782 (5)	-0.4051 (8)
C15	0.3980 (6)	0.3691 (6)	-0.5135 (7)
C16	0.5573 (8)	0.1638 (7)	-0.4954 (11)

The ^1H NMR spectra of complexes **2a,b** exhibit equivalent Cp or Cp′ ligands, and the two *p*-tolyl substituents of the alkyne are also equivalent. The ^1H NMR resonances of the Cp or Cp′ ligands in the reduced Nb(II) complexes **2a,b** are shifted upfield by about 0.5 ppm with respect to those of their respective Nb(III) precursors, reflecting the change in oxidation state of the metal. The alkyne carbon resonances of **2a** and **2b**, at δ 213.9 and 216.4, respectively, are characteristic of four-electron-donor alkynes and very close to the values found for the Nb(III) complexes $CpNbCl_2(ArCCAr)$. The ^{13}C NMR resonances of the alkyne carbons are hardly affected by the change in oxidation state.

The molecular structures of 1 and **2a** are shown in Figures 1 and 2. Final positional parameters for all non-hydrogen atoms are reported in Tables II and IV. Selected bond distances and angles are summarized in Tables III and V. The Nb(II) d^3–d^3 dimer 1 is diamagnetic, and the Nb–Nb distance of 3.0567 (1) Å is commensurate with a distance expected for a Nb–Nb single bond, more than 1 Å shorter than the M–M nonbonded

Table III. Bond Distances (Å) and Selected Bond Angles (deg) for [Cp′Nb(μ-Cl)(CO)$_2$]$_2$ (1)

	Bond Distances		
Nb1–Nb2	3.056 (1)	Nb1–Cl1	2.559 (1)
Nb1–Cl2	2.560 (1)	Nb1–C1	2.068 (6)
Nb1–C2	2.081 (5)	Nb2–Cl1	2.566 (1)
Nb2–Cl2	2.561 (1)	Nb2–C3	2.093 (5)
Nb2–C4	2.067 (5)	Nb1–C5	2.457 (5)
Nb1–C6	2.419 (5)	Nb1–C7	2.340 (5)
Nb1–C8	2.314 (5)	Nb1–C9	2.366 (5)
Nb2–C11	2.429 (5)	Nb2–C12	2.416 (5)
Nb2–C13	2.342 (5)	Nb2–C14	2.312 (5)
Nb2–C15	2.353 (5)	O1–C1	1.150 (6)
O2–C2	1.131 (6)	O3–C3	1.125 (6)
O4–C4	1.130 (6)	C5–C10	1.500 (8)
C5–C6	1.396 (8)	C6–C7	1.406 (8)
C7–C8	1.411 (8)	C8–C9	1.423 (8)
C9–C5	1.441 (8)	C11–C16	1.493 (9)
C11–C12	1.386 (8)	C12–C13	1.391 (8)
C13–C14	1.400 (8)	C14–C15	1.404 (9)
C15–C11	1.425 (8)		
	Bond Angles		
Cl1–Nb1–Cl2	74.81 (5)	Cl2–Nb2–Cl1	74.67 (5)
Nb1–Cl1–Nb2	73.19 (4)	Nb1–Cl2–Nb2	73.26 (4)
C1–Nb1–C2	82.1 (2)	C3–Nb2–C4	83.6 (2)
Nb1–Nb2–C3	89.2 (2)	Nb2–Nb1–C1	84.4 (2)
Nb1–Nb2–C4	84.4 (2)	Nb2–Nb1–C2	88.0 (1)
Nb1–Nb2–Cl1	53.30 (3)	Nb2–Nb1–Cl1	53.51 (3)
Nb1–Nb2–Cl2	53.36 (3)	Nb2–Nb1–Cl2	53.38 (3)
Nb1–C1–O1	172.6 (5)	Nb1–C2–O2	175.6 (5)
Nb2–C3–O3	176.4 (7)	Nb2–C4–O4	172.2 (5)

Table IV. Fractional Atomic Coordinates for [Cp′Nb(μ-Cl)(MePhC≡CPhMe)]$_2$ (2a)

atom	x	y	z	U, Å^2
Nb	0.4807 (1)	0.1490 (1)	1.0624 (1)	0.0331
Cl	0.3266 (1)	0.1174 (1)	0.8504 (1)	0.0374
C10	0.6099 (5)	0.2189 (4)	0.9968 (3)	0.0343
C20	0.6740 (5)	0.2112 (4)	1.1139 (3)	0.0381
C11	0.6494 (5)	0.2451 (4)	0.9000 (3)	0.0334
C12	0.5228 (5)	0.3273 (5)	0.7914 (4)	0.0436
C13	0.5658 (6)	0.3448 (5)	0.7001 (4)	0.0543
C14	0.7331 (7)	0.2801 (6)	0.7121 (4)	0.0644
C15	0.8594 (6)	0.1988 (5)	0.8198 (4)	0.0546
C16	0.8178 (5)	0.1850 (4)	0.9126 (4)	0.0399
C17	0.7771 (9)	0.2956 (8)	0.6105 (5)	0.1070
C21	0.8039 (5)	0.2433 (5)	1.2085 (3)	0.0415
C22	0.8812 (6)	0.1706 (5)	1.3233 (4)	0.0554
C23	1.0058 (6)	0.1988 (6)	1.4118 (4)	0.0567
C24	1.0544 (5)	0.3020 (5)	1.3894 (4)	0.0516
C25	0.9762 (6)	0.3750 (5)	1.2755 (4)	0.0602
C26	0.8545 (5)	0.3455 (5)	1.1863 (4)	0.0512
C27	1.1892 (6)	0.3345 (7)	1.4869 (5)	0.0707
Cp1	0.3763 (6)	0.1638 (5)	1.2240 (4)	0.0532
Cp2	0.2466 (6)	0.1789 (5)	1.1137 (4)	0.0587
Cp3	0.1966 (5)	0.3170 (5)	1.0501 (4)	0.0494
Cp4	0.2998 (6)	0.3837 (5)	1.1184 (4)	0.0525
Cp5	0.4127 (6)	0.2892 (5)	1.2253 (4)	0.0508
Cp6	0.4554 (8)	0.0436 (6)	1.3240 (5)	0.0874

Table V. Bond Distances (Å) and Selected Bond Angles (deg) for [Cp′Nb(μ-Cl)(MePhC≡CPhMe)]$_2$ (2a)[a]

	Bond Distances		
Nb–Nb*	3.073 (1)	Nb–Cl	2.501 (1)
Nb–Cl*	2.431 (1)	Nb–C10	2.087 (4)
Nb–C20	2.068 (4)	C10–C11	1.458 (5)
C10–C20	1.314 (5)	C11–C12	1.393 (5)
C20–C21	1.466 (5)	C12–C13	1.386 (6)
C11–C16	1.390 (5)	C14–C15	1.384 (6)
C13–C14	1.378 (6)	C15–C16	1.382 (6)
C14–C17	1.504 (6)	C21–C26	1.388 (5)
C21–C22	1.391 (6)	C23–C24	1.383 (6)
C22–C23	1.382 (6)	C24–C27	1.514 (6)
C24–C25	1.382 (6)	C25–C26	1.374 (6)
	Bond Angles		
Cl–Nb–Cl*	102.9 (1)	Nb–Cl–Nb*	77.1 (1)
Nb–Nb*–Cl	52.48 (4)	Nb–Nb*–Cl*	50.44 (3)
Nb*–Nb–C10	100.3 (1)	Nb*–Nb–C20	119.6 (1)
C10–Nb–C20	36.9 (1)	Nb–C10–C20	70.8 (2)
Nb–C20–C10	72.4 (2)	Nb–C10–C11	151.7 (3)
Nb–C20–C21	149.6 (3)	C20–C10–C11	136.9 (3)
C10–C20–C21	137.9 (4)		

[a] Asterisks denote symmetry-related atoms.

distance in the Nb(III) dimer [Cp′Nb(μ-Cl)(CO)$_2$]$_2$.[10] The CO ligands are terminal (this is consistent with the IR spectrum) and are almost eclipsed in the structure, although there is a small torsion around the Nb1–Nb2 axis that is probably caused by ligand–ligand repulsions. The average Nb–Cl distance is 2.56 Å, and the Nb–μ-Cl–Nb angle is 73.2 (1)°, almost 30° more acute than in [Cp′Nb(μ-Cl)(CO)$_2$]$_2$.

In contrast with the structure of 1, the Nb$_2$Cl$_2$ core of **2a** is strictly planar. The Nb$_2$Cl$_2$ core has the shape of a rhombus compressed in the Nb–Nb′ direction. The Nb(II) d^3–d^3 dimer **2a** is diamagnetic and has a Nb–Nb′ distance of 3.073 (1) Å, consistent with a M–M single bond. The Nb–Cl–Nb′ angle is 77.1 (1)°, about 24° more acute than the μ-Cl–Nb–μ-Cl angle (102.9 (1)°). The 4e-donor alkynes are strongly bonded to the metal with M–C distances of 2.087 (4) and 2.068 (4) Å, comparable to the niobium–alkyne carbon distances in the Nb(III) complex Cp′NbCl$_2$(ArC≡CAr) (2.063 (5) and 2.079 (5) Å). The alkyne C–C distance in **2a** is 1.314 (5) Å, somewhat longer than that in Cp′NbCl$_2$(ArC≡CAr) (1.307 (6) Å), but the difference is not statistically significant. These structural data plus the similar chemical shifts of the alkyne carbons in the ^{13}C NMR spectra of Cp′NbCl$_2$(ArC≡CAr) and **2a** indicate that reduction of the niobium by one electron did not significantly affect the metal–alkyne bond; the ligand is still a strongly bound, 4e-donor alkyne. A plausible explanation is that the added electron occupies an orbital (M–M bonding) that is not involved in metal–alkyne bonding.

Interestingly, the alkyne ligands in **2a** are terminal. In most (if not all) known transition-metal-bonded dimers with alkyne ligands, the alkynes assume a bridging position.[11] It is convenient to consider 1 and **2a** as M–M-bonded dimers to explain in a simple manner their diamagnetism and the structural data. However, bridged dimers always present the problem of deciding whether or not there is a *direct* bonding interaction of primarily metal-centered orbitals or interaction through the ligands.[12] The preference for terminal vs bridge position, and for coupled vs uncoupled alkynes, for example as in Cp$_2$Mo$_2$Cl$_2$(μ-η^4-C$_4$R$_4$),[13] has been explored with Fenske–Hall calculations. The results will be reported elsewhere.[14]

Herrmann and co-workers[15] have reported the structures of [CpNb(μ-S)(CO)$_2$]$_2$ and [CpNb(μ-SCH$_3$)(CO)$_2$]$_2$, isolated from the reactions of CpNb(CO)$_4$ with H$_2$S and CH$_3$SH, respectively. The structures of these two sulfur-bridged compounds and 1 are very similar. Because of the similarity among the three complexes we concur with a pre-

---

[11] Hoffman, D. M.; Hoffmann, R.; Fisel, C. R. *J. Am. Chem. Soc.* **1982**, *104*, 3858.

[12] (a) Summerville, R. H.; Hoffmann, R. *J. Am. Chem. Soc.* **1976**, *98*, 7240. (b) Kostic, N. M.; Fenske, R. F. *Inorg. Chem.* **1983**, *22*, 666. (c) Hay, P. J.; Thibeault, J.-C.; Hoffmann, R. *J. Am. Chem. Soc.* **1975**, *97*, 4884. (d) Shaik, S.; Hoffmann, R. *J. Am. Chem. Soc.* **1980**, *102*, 1194. (e) Shaik, S.; Hoffmann, R.; Fisel, C. R.; Summerville, R. H. *J. Am. Chem. Soc.* **1980**, *102*, 4555. (f) Bottomley, F. *Inorg. Chem.* **1983**, *22*, 2656. (g) Pinhas, A. R.; Hoffmann, R. *Inorg. Chem.* **1979**, *18*, 654.

[13] Hirpo, W.; Curtis, M. D. *J. Am. Chem. Soc.* **1988**, *110*, 5218.

[14] Milletti, M. C.; Curtis, M. D. *Polyhedron*, in press.

[15] Herrmann, W. A.; Biersack, H.; Ziegler, M. L.; Balbach, B. *J. Organomet. Chem.* **1981**, *206*, C33.

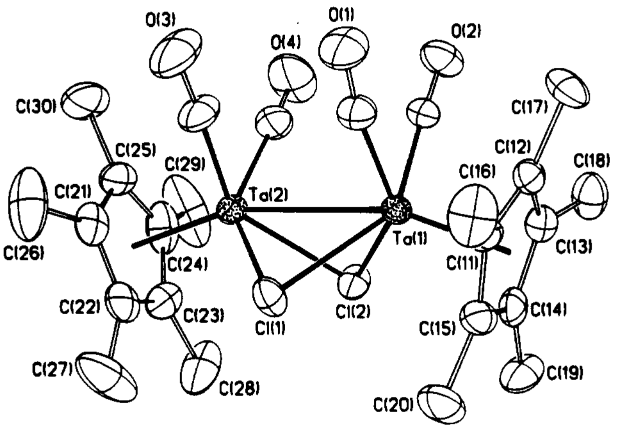

Figure 3. ORTEP plot of the molecular structure of [(C_5Me_5)Ta(μ-Cl)$(CO)_2$]$_2$ (3) with the numbering scheme.

vious suggestion[16] that the reported sulfido-bridged complex [CpNb(μ-S)$(CO)_2$]$_2$ is actually a hydrosulfido complex, [CpNb(μ-SH)$(CO)_2$]$_2$.

The reductions of [CpNbCl(μ-Cl)$(CO)_2$]$_2$ and CpNbCl_2(ArCCAr) with 2 equiv of sodium amalgam were studied in an effort to obtain Nb(I), d^4 dimers that could exhibit Nb=Nb double bonds. The reaction of the carbonyl complex [CpNbCl(μ-Cl)$(CO)_2$]$_2$ with 2 equiv or more of sodium amalgam gave an insoluble, black, intractable material that contained no CO. It is surprising that reduction should cause loss of CO, since in most known niobium carbonyl complexes the metal has an oxidation state of +1 or lower. Some decarbonylation was also observed in the preparation of 1.

Reaction of the alkyne complex Cp′NbCl_2(ArC≡CAr) with 2 equiv of sodium amalgam in toluene for 24 h afforded a small yield of **2a** and a dark uncharacterizable material.

The tantalum alkyne complexes CpTaCl_2(ArCCAr) were not reduced cleanly with sodium amalgam. Proton NMR analysis of the products revealed peaks for the starting material and several peaks in the Cp region, indicating that a mixture of products was obtained.

(Pentamethylcyclopentadienyl)tantalum(III) complexes Cp*Ta$Cl_2$$(CO)_2$(THF) and Cp*Ta$Cl_2$(PhCCPh) are available from the reduction of Cp*TaCl_4 with Al/HgCl_2 in high yield.[17] Na/Hg reduction of Cp*Ta$Cl_2$$(CO)_2$(THF) gave the brown crystalline product [Cp*Ta(μ-Cl)$(CO)_2$]$_2$ (3) in high yield according to eq 4.

$$2\mathrm{Cp^*TaCl_2(CO)_2(THF)} \xrightarrow{2\mathrm{Na/Hg}} \underset{\mathbf{3}}{[\mathrm{Cp^*Ta}(\mu\text{-Cl})(\mathrm{CO})_2]_2} \qquad (4)$$

Table VI. Fractional Atomic Coordinates for [(η^5-C_5Me_5)Ta(μ-Cl)$(CO)_2$]$_2$ (3)

atom	x	y	z	U, Å^2
Ta1	0.40943 (4)	0.9778 (3)	0.21067 (2)	0.0346
Ta1	0.34616 (5)	0.20273 (3)	0.8374 (2)	0.0385
Cl1	0.1916 (3)	0.2088 (2)	0.1766 (1)	0.0509
Cl2	0.2704 (3)	0.0410 (2)	0.1027 (1)	0.0488
O1	0.6410 (11)	0.2518 (6)	0.2745 (4)	0.078
O2	0.7414 (9)	0.0372 (6)	0.1764 (4)	0.071
O3	0.5863 (15)	0.3509 (8)	0.1472 (6)	0.126
O4	0.6599 (12)	0.1236 (10)	0.0447 (6)	0.126
C1	0.5501 (13)	0.2011 (8)	0.2486 (6)	0.055
C2	0.6193 (11)	0.0575 (7)	0.1839 (5)	0.049
C3	0.4992 (16)	0.2959 (9)	0.1269 (6)	0.073
C4	0.5506 (14)	0.1503 (10)	0.0608 (7)	0.073
C11	0.3822 (11)	0.0863 (7)	0.3202 (5)	0.043
C12	0.5140 (12)	0.0309 (7)	0.3091 (5)	0.044
C13	0.4520 (12)	−0.0415 (7)	0.2660 (5)	0.045
C14	0.2862 (13)	−0.0319 (7)	0.2544 (5)	0.050
C15	0.2446 (12)	0.0475 (8)	0.2879 (5)	0.050
C16	0.3937 (18)	0.1597 (9)	0.3722 (6)	0.076
C17	0.6773 (14)	0.0379 (10)	0.3461 (6)	0.073
C18	0.5416 (17)	−0.1248 (9)	0.2477 (7)	0.073
C19	0.1726 (16)	−0.0977 (9)	0.2171 (6)	0.075
C20	0.0791 (14)	0.0814 (11)	0.2921 (7)	0.076
C21	0.2501 (15)	0.3362 (8)	0.0294 (5)	0.057
C22	0.1169 (15)	0.2785 (9)	0.0259 (6)	0.064
C23	0.1413 (15)	0.2027 (9)	−0.0086 (5)	0.067
C24	0.2894 (19)	0.2077 (9)	−0.0295 (6)	0.079
C25	0.3584 (14)	0.2933 (9)	−0.0045 (6)	0.064
C26	0.2513 (27)	0.4305 (10)	0.0561 (8)	0.116
C27	0.0291 (19)	0.2994 (15)	0.0542 (8)	0.130
C28	0.0254 (23)	0.1244 (11)	−0.0262 (9)	0.129
C29	0.3464 (28)	0.1459 (14)	−0.0774 (7)	0.143
C30	0.5006 (19)	0.3410 (14)	−0.0256 (9)	0.123

Table VII. Bond Distances (Å) and Selected Bond Angles (deg) for [(η^5-C_5Me_5)Ta(μ-Cl)$(CO)_2$]$_2$ (3)

Bond Distances			
Ta1–Ta2	3.062 (1)	Ta1–Cl1	2.521 (3)
Ta1–Cl2	2.543 (2)	Ta1–C1	2.038 (11)
Ta1–C2	2.071 (11)	Ta1–C11	2.354 (10)
Ta1–C12	2.345 (10)	Ta1–C13	2.366 (10)
Ta1–C14	2.441 (11)	Ta1–C15	2.435 (11)
Ta2–Cl1	2.531 (3)	Ta2–Cl2	2.528 (3)
Ta2–C3	2.028 (13)	Ta2–C4	2.056 (14)
Ta2–C21	2.366 (11)	Ta2–C22	2.436 (12)
Ta2–C23	2.420 (11)	Ta2–C24	2.356 (12)
Ta2–C25	2.304 (13)	O1–C1	1.161 (14)
O2–C2	1.133 (13)	O3–C3	1.146 (17)
O4–C4	1.124 (18)	C11–C12	1.452 (14)
C11–C15	1.401 (14)	C11–C16	1.533 (16)
C12–C13	1.452 (14)	C12–C17	1.509 (15)
C13–C14	1.426 (15)	C13–C18	1.536 (17)
C14–C15	1.443 (16)	C14–C19	1.515 (17)
C15–C20	1.530 (17)	C21–C22	1.427 (18)
C21–C25	1.412 (18)	C21–C26	1.503 (19)
C22–C23	1.369 (18)	C22–C27	1.511 (22)
C23–C24	1.419 (21)	C23–C28	1.539 (22)
C24–C25	1.463 (19)	C24–C29	1.497 (24)
C25–C30	1.542 (22)		

Bond Angles			
Ta2–Ta1–Cl1	52.8 (1)	Ta2–Ta1–Cl2	52.6 (1)
Cl1–Ta1–Cl2	74.3 (1)	Ta1–Ta2–Cl1	52.5 (1)
Ta1–Ta2–Cl2	53.1 (1)	Cl1–Ta2–Cl2	74.4 (1)
Ta2–Ta1–C1	88.7 (3)	Ta2–Ta1–C2	87.5 (3)
Ta1–Ta2–C3	86.4 (4)	Ta1–Ta2–C4	88.1 (4)
C3–Ta2–C4	80.4 (5)	C1–Ta1–C2	79.9 (4)
Ta2–C3–O3	175 (1)	Ta2–C4–O4	176 (1)
Ta1–C1–O1	172 (1)	Ta1–C2–O2	172 (1)

^{1}H and ^{13}C nuclei in the methyl groups resonate at δ 1.74 and 11.3, respectively. The molecule displays a parent ion (m/e 814) and clean fragmentation patterns in the mass spectrum. Two IR bands at 1976 and 1893 cm^{-1} show that the carbonyls are strongly bonded to the tantalum. They are not replaced with other neutral ligands, e.g. PMe$_3$ or alkynes, at room temperature. The molecular structure of **3** is shown in Figure 3. Final positional parameters for all non-hydrogen atoms and selected bond distances and angles are listed in Tables VI and VII, respectively. The

---

(16) Skripkin, Yu. V.; Eremenko, I. L.; Pasynskii, A. A.; Struchkov, Yu. T.; Shklover, V. E. *J. Organomet. Chem.* **1984**, *267*, 285. Although Herrmann et al.[15] measured both the IR and NMR spectra of the putative sulfide complexes, either measurement could easily have missed the SH group. The S–H stretching modes are often very weak, and traces of acids or bases in the solution could lead to exchange broadening and collapse of the SH absorption in the ^{1}H NMR spectrum. A further argument in support of Skripkin et al.'s formulation of the reported[15] [CpNb$(CO)_2$]$_2$(μ-S)$_3$ as [CpNb$(CO)_2$]$_2$(μ-S)(μ-SH)$_2$ is that the Nb atoms in the original (μ-S)$_3$ formulation would be Nb(IV) (d^1) and no stable transition-metal carbonyls have a d electron:CO ratio as low as 1:2. This ratio is normally closer to unity and is never below 2:3.

(17) Kwon, D.; Curtis, M. D. *Organometallics* **1990**, *9*, 1.

(18) *International Tables for X-ray Crystallography*; Kynoch Press: Birmingham, England, 1974.

crystal structure of **3** is basically the same as that of $Cp_2Nb_2(\mu\text{-}Cl)_2(CO)_4$,[10] where the core is butterfly-shaped.

The reduction of $Cp^*TaCl_2(PhCCPh)$ in THF is rather messy, but in toluene two products are formed cleanly in comparable yields. Spectroscopic and analytical data show these are isomeric dimers with the formula $[Cp^*TaCl(PhCCPh)]_2$. X-ray-quality crystals have not been obtained to date. Work is continuing on these compounds, and the results will be reported later.

The differences between the structures of the carbonyl dimers **1** and **3** and the alkyne dimer **2** are striking. The former have a deeply folded Nb_2Cl_2 core that eclipses the two sets of carbonyl groups on each metal, while in **3** the Nb_2Cl_2 core is planar and the coordinated acetylenes are transoid. The cisoid arrangements in the carbonyl complexes place the π-donor chlorides trans to the π-acceptor carbonyls, an understandable arrangement that leads to increased synergic bonding. But the alkyne group is known to be a powerful electron acceptor also, especially in early-transition-metal complexes. So why are the structures so different?

A possible explanation arises from the difference in the symmetry of the lowest energy acceptor orbitals between a *cis*-$(CO)_2$ grouping and the RCCR group. Figure 4 of ref 10a shows the LUMO's of $CpNbCl_2(PH_3)_2$ and $CpNbCl_2(RCCR)$ fragments. In the phosphine complex, the LUMO is a d_{z^2} orbital directed down between the legs of the four-legged piano stool. Adding an electron to the LUMO to make a Nb(II) radical would lead to a Nb–Nb bond along the *z* axis and give the highly folded structure observed. (The two chloride ligands of each "$CpNbCl_2L_2$" fragment are shared, but this does not disturb the symmetry of the metal fragment.) Conversely, the LUMO of the $CpNbCl_2(RCCR)$ fragment is an $x^2 - y^2$ orbital pointing *between* the chloride ligands. Formation of a Nb–Nb bond with this orbital will give rise to the planar Nb_2Cl_2 core. Thus, if the LUMO of a $CpNbCl_2(CO)_2$ fragment resembles that of $CpNbCl_2(PH_3)_2$, the different Nb(II) structures can be readily rationalized. See ref 10a for a fuller description of the symmetry properties of the ligands that lead to the different LUMO's.

The homometallic dimers **1**–**3** provide examples of niobium and tantalum complexes in the relatively rare +2 oxidation state, and they are promising starting points for the study of the chemistry of Nb(II) and Ta(II) complexes with carbonyl and alkyne ligands.

Acknowledgment. We thank the donors of the Petroleum Research Fund, administered by the American Chemical Society, and the National Science Foundation (Grant CHE-8619864) for support of this research.

Supplementary Material Available: Tables VIIIS–XS (thermal parameters for **1**, **2a**, and **3**) and Tables XIS–XIIIS (bond angles for **1**, **2a**, and **3**) (5 pages); Tables XIVS–XVIS (F_o vs F_c for **1**, **2a**, and **3**) (45 pages). Ordering information is given on any current masthead page.

Photoelectron Spectroscopy and Rates of CO Substitution of $(\eta^5\text{-}C_5H_4X)Rh(CO)_2$ Compounds. Separation of σ and π Ring Substituent Effects

Dennis L. Lichtenberger* and Sharon K. Renshaw

Laboratory for Electron Spectroscopy and Surface Analysis, Department of Chemistry,
The University of Arizona, Tucson, Arizona 85721

Fred Basolo* and Minsek Cheong

Department of Chemistry, Northwestern University, Evanston, Illinois 60208

Received April 9, 1990

The He I photoelectron spectra for a series of monosubstituted $(\eta^5\text{-}C_5H_4X)Rh(CO)_2$ compounds are reported (where X = NO_2, CF_3, Cl, H, CH_3, NMe_2) and compared to the rates of carbonyl substitution reactions. The carbonyl substitution by phosphine follows an associative mechanism, and the rates are generally inhibited by greater electron richness at the metal center in these compounds. However, the rates for certain substitutions, particularly when X is Cl or NMe_2, are faster than indicated by the inductive characteristics of these groups. The photoelectron spectra of the $(\eta^5\text{-}C_5H_4X)Rh(CO)_2$ compounds illustrate the effects of X on the electronic structure and rates of substitution. Pronounced shifts are seen in the cyclopentadienyl π and metal d valence ionizations as the X group is varied. The shifts of most of the valence ionizations closely follow the inductive capabilities of the X substituents, as also indicated by correlations with Hammett σ values and the carbonyl stretching frequencies of the compounds. Certain ionizations are also affected by orbitals of the X group that have π symmetry with respect to the cyclopentadienyl ring. Thus, the ionization energy shifts provide a relative measure of the inductive and resonance (π) interaction between X and the compound. The rates of CO substitution correlate with the ionizations when the shifts due to both the inductive and resonance (π) effects are taken into account. These results suggest that the "slipped ring" intermediate $(\eta^3\text{-}C_5H_4X)Rh(CO)_2PPh_3$ is stabilized through π delocalization on the cyclopentadienyl ring, thus enhancing the rates of substitution.

Introduction

Associative substitution in 18-electron organometallic compounds can be facilitated if a pair of electrons is easily localized on a ligand, thereby releasing a coordination site at the metal.[1] If the molecule contains a cyclopentadienyl ring (Cp), one mechanism for freeing a coordination site is for the Cp ring to "slip" from η^5 to η^3 coordination, leaving the other two Cp π electrons localized in a carbon–carbon bond:[2]

---

* To whom correspondence should be addressed.

[1] (a) Basolo, F. *Inorg. Chim. Acta* **1985**, *100*, 33. (b) Basolo, F. *Inorg. Chim. Acta* **1981**, *50*, 65.

0276-7333/91/2310-0148$02.50/0